

Design and Synthesis of Novel Insecticides Based on the Serotonergic Ligand 1-[(4-Aminophenyl)ethyl]-4-[3-(trifluoromethyl)phenyl]piperazine (PAPP)[†]

MINGYI CAI, ZHONG LI,* FENG FAN, QINGCHUN HUANG, XUSHENG SHAO, AND GONGHUA SONG*

Shanghai Key Laboratory of Chemical Biology, School of Pharmacy, East China University of Science and Technology, P.O. Box 544, 130 Meilong Road, Shanghai 200237, People's Republic of China

1-[(4-Aminophenyl)ethyl]-4-[3-(trifluoromethyl)phenyl]piperazine (PAPP) is a 5-HT_{1A} agonist and was reported to display high affinity for serotonin (5-HT) receptor from the parasitic nematode *Haemonchus contortus*. The present investigation explored the possibility of using PAPP as a lead compound of new insecticides with novel mode of action. On the basis of the PAPP scaffold, a series of 1-arylmethyl-4-[(trifluoromethyl)pyridin-2-yl]piperazine derivatives were designed, synthesized, and evaluated for biological activities against the armyworm *Pseudaletia separata* (Walker). Bioassays showed that most of the target compounds displayed certain growth-inhibiting activities or larvicidal activities against armyworm. The quantitative structure–activity relationship (QSAR) for growth-inhibiting activities was also analyzed and established.

KEYWORDS: PAPP; 1-arylmethyl-4-[(trifluoromethyl)pyridin-2-yl]piperazine; larvicidal activity; growth inhibiting activity; QSAR

INTRODUCTION

As one of the main pest management tools, insecticides play a very important role in modern agriculture. However, the frequent and wide application of traditional insecticides has brought about an inevitable problem, namely, the occurrence and development of resistance of pest species. Therefore, it is critically necessary to discover new insecticidal candidates with novel modes of action.

In invertebrate species, serotonin [5-hydroxytryptamine (5-HT)] as a significant monoamine neurotransmitter is widely distributed throughout the central and peripheral nervous systems and involved in a number of physiological processes such as feeding, procreation, and development (1–7). Some 5-HT receptors (5-HTRs) have already been cloned from *Drosophila*, molluscs, and nematodes. It is interesting that most of them show relatively low affinities with serotonin with the exception of the 5-HT_{1Hc} receptor from the parasitic nematode *Haemonchus contortus*. The 5-HT_{1Hc} receptor displayed nanomolar binding affinity for serotonin and serotonergic ligands. Such a unique pharmacological profile was distinct from the other known invertebrate and mammalian 5-HT receptors (8, 9).

It has been found that many N¹-substituted N⁴-arylpiperazine derivatives, for example, PAPP, BMY7378, and NAN-190 (Table 1), showed high affinities and good selectivity for 5-HTRs with the incorporation of the appropriate N¹- and N⁴-substituent groups (9–12). Among those notable serotonergic ligands, PAPP, a N¹-arylated alkyl N⁴-arylpiperazine derivative, exhibited the highest affinity with 5-HT_{1Hc} receptor as shown in Table 1 (9)

according to Smith et al.'s testing results. Thus, it might be reasonable to regard PAPP as a potential lead compound for discovering insecticidal candidates with a novel mode of action.

To validate the hypothesis, the structural motif of PAPP was shared involving the introduction of appropriate N¹- and N⁴-substituent groups for agrochemicals by the following two ways. First, owing to the successful application in neonicotinoids, arylmethyl groups might be adopted as profitable N¹-substituent groups. Second, due to the unique bioactivities in the agrochemicals (i.e., herbicides fluzifog-P-butyl and haloxyfog and insecticides fluzuron and chlorfluzuron), the trifluoromethylpyridine ring might be a good candidate as the N⁴-substituent group. Therefore, a series of 1-arylmethyl-4-[(trifluoromethyl)pyridin-2-yl]piperazine derivatives (Scheme 1) were designed, synthesized (Scheme 2), and bioassayed. It was found that most of the target compounds exhibited certain growth-inhibiting activities or larvicidal activities against the armyworm *Pseudaletia separata* (Walker). This result verified that PAPP could become a competent lead compound for the development of new insecticides.

MATERIALS AND METHODS

Synthesis. All chemicals or reagents were purchased from standard commercial suppliers. Analytical thin-layer chromatography (TLC) was carried out on precoated silica gel (SiO₂) plates (60 F₂₅₄). Melting points were determined on a Büchi B540 (Büchi Labortechnik AG, Flawil, Switzerland) and are uncorrected. The infrared spectra were recorded on a Nicolet 470 IR Fourier transform spectrometer in KBr pellets. ¹H NMR spectra were recorded on a Bruker WP-500SY (500 MHz) spectrometer in CDCl₃ with TMS as an internal standard. High-resolution mass spectra were obtained on a MicroMass GCT CA 055 spectrometer.

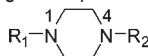
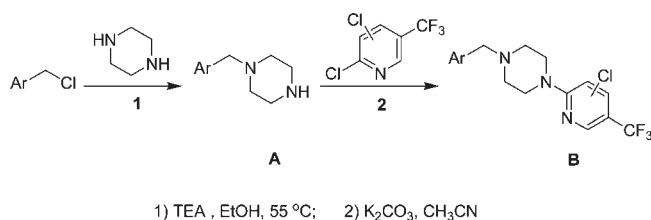
[†]Part of the ECUST-Qian Pesticide Cluster.

*Authors to whom correspondence should be addressed [e-mail (Z.L.) lizhong@ecust.edu.cn or (G.S.) ghsong@ecust.edu.cn].

Table 1. Affinities of N¹-Substituted N⁴-Arylpiperazine Derivatives Binding to the Cloned 5-HT_{1Hc} Receptor of the Parasitic Nematode *Haemonchus contortus* Reported by Smith et al. (9)

Compounds	Chemical Structures	K _i ^a (nM)
Serotonin		0.8
PAPP		0.4
BMY7378		3.6
NAN-190		7.7

^a K_i values (nM) for [³H]-serotonin binding to Sf9 cell membranes expressing the Parasitic nematode *Haemonchus contortus* 5-HT_{1Hc} receptor.

Scheme 1. Structure of Target Compounds**Scheme 2.** Synthesis of Target Compounds B

General Synthetic Procedure for the Target Compounds. To a warm (oil bath temperature ca. 50 °C) solution of piperazine (4.0 mmol) and triethylamine (3.0 mmol) in EtOH (30 mL) was added dropwise aryl chloromethane (2.0 mmol) in ethanol (15 mL), and then the reaction mixture was allowed to stir at 55 °C for 12 h. After the reaction finished, the solvent was removed under vacuum. The oily residue was treated with water (15 mL) and extracted with CH₂Cl₂ (4 × 15 mL). The combined extracts were washed with water, dried over anhydrous Na₂SO₄, and concentrated. The residue was purified by flash column chromatography on silica gel with CH₂Cl₂/EtOH (10:1 v/v) to obtain 1-(arylmethyl)piperazine (A) in 80–86% yield.

Equimolar amounts (2.0 mmol) of 1-(arylmethyl)piperazine (A), anhydrous K₂CO₃, and 2,3-dichloro-5-(trifluoromethyl)pyridine (or 6-chloro-3-(trifluoromethyl)pyridine) in MeCN (20 mL) were stirred at 55 °C for 10 h. After cooling, the reaction mixture was treated with water (15 mL) and extracted with EtOAc (4 × 15 mL). The combined extracts were washed with water (10 mL) and brine (10 mL), dried over anhydrous Na₂SO₄, and concentrated. The residue was purified by flash column chromatography on silica gel with petroleum ether/EtOAc (4:1 v/v) to yield the desired product (B).

When 2,6-dichloro-3-(trifluoromethyl)pyridine was used, the reaction mixture was stirred at 45 °C for 10 h. The 6-substituted products as the major reaction products were formed along with minor 2-substituted impurities, which could be removed later by column chromatography.

Compounds C₁ and C₂ were synthesized in a similar way.

1-(4-Chlorobenzyl)-4-[5-(trifluoromethyl)pyridin-2-yl]piperazine (B₁): yield, 75%; white solid; mp, 91–92 °C; IR (KBr) ν 2797, 1610, 1507, 1300, 1109, 815 cm⁻¹; ¹H NMR (500 MHz, CDCl₃) δ 2.52–2.54 (m, 4H, pip-H), 3.53 (s, 2H, CH₂), 3.64–3.66 (m, 4H, pip-H), 6.62 (d, J = 9.01 Hz, 1H, Py-H), 7.30–7.34 (m, 4H, Ar-H), 7.61–7.62 (m, 1H, Py-H), 8.39 (s, 1H, Py-H); EI-MS, m/z (%) 355 (6, M⁺), 209 (4), 193 (16), 180 (34), 175 (37), 168 (8), 125 (100), 56 (10). HRMS (EI⁺) calcd for C₁₇H₁₇ClF₃N₃, 355.1063; found, 355.1064.

1-[(6-Chloropyridin-3-yl)methyl]-4-[5-(trifluoromethyl)pyridin-2-yl]piperazine (B₂): yield, 73%; yellow solid; mp, 88–89 °C; IR (KBr) ν 2806, 1606, 1500, 1374, 1118, 817 cm⁻¹; ¹H NMR (500 MHz, CDCl₃) δ 2.53–2.55 (m, 4H, pip-H), 3.54 (s, 2H, CH₂), 3.65–3.66 (m, 4H, pip-H), 6.64 (d, J = 9.02 Hz, 1H, Py-H), 7.33–7.34 (m, 1H, Py-H), 7.62 (dd, J_1 = 2.25 Hz, J_2 = 2.24 Hz, 1H, Py-H), 7.70 (dd, J_1 = 2.25 Hz, J_2 = 2.29 Hz, 1H, Py-H), 8.34 (s, 1H, Py-H), 8.38 (s, 1H, Py-H); EI-MS, m/z (%) 356 (12, M⁺), 337 (7), 230 (10), 194 (28), 175 (100), 147 (25), 126 (67), 56 (23). HRMS (EI⁺) calcd for C₁₆H₁₆ClF₃N₄, 356.1016; found, 356.1037.

1-[(2-Chlorothiazol-5-yl)methyl]-4-[5-(trifluoromethyl)pyridin-2-yl]piperazine (B₃): yield, 72%; yellow solid; mp, 61–62 °C; IR (KBr) ν 2813, 1613, 1414, 1328, 1119, 811 cm⁻¹; ¹H NMR (500 MHz, CDCl₃) δ 2.59–2.61 (m, 4H, pip-H), 3.65–3.67 (m, 4H, pip-H), 3.71 (s, 2H, CH₂), 6.63 (d, J = 9.02 Hz, 1H, Py-H), 7.38 (s, 1H, thiazol-H), 7.63 (dd, J_1 = 2.24 Hz, J_2 = 2.25 Hz, 1H, Py-H), 8.39 (s, 1H, Py-H); EI-MS, m/z (%) 362 (12, M⁺), 327 (14), 230 (7), 201 (8), 187 (21), 175 (100), 165 (14), 131 (31), 56 (10). HRMS calcd for C₁₄H₁₄ClF₃N₄S, 362.0580; found, 362.0583.

1-(2-Chlorobenzyl)-4-[3-chloro-5-(trifluoromethyl)pyridin-2-yl]piperazine (B₄): yield, 72%; white solid; mp, 7071 °C; IR (KBr) ν 2823, 1606, 1329, 1117, 776 cm⁻¹; ¹H NMR (500 MHz, CDCl₃) δ 2.67–2.69 (m, 4H, pip-H), 3.55–3.57 (m, 4H, pip-H), 3.70 (s, 2H, CH₂), 7.23–7.25 (m, 2H, Ar-H), 7.37 (d, J = 7.65 Hz, 1H, Ar-H), 7.50–7.51 (m, 1H, Ar-H), 7.74 (d, J = 1.71 Hz, 1H, Py-H), 8.39 (s, 1H, Py-H); EI-MS, m/z (%) 389 (M⁺), 221 (5), 193 (11), 180 (100), 168 (18), 125 (67), 56 (7). HRMS (EI⁺) calcd for C₁₇H₁₆Cl₂F₃N₃, 389.0673; found, 389.0682.

1-(4-Chlorobenzyl)-4-[3-chloro-5-(trifluoromethyl)pyridin-2-yl]piperazine (B₅): yield, 72%; yellow oil; IR (KBr) ν 2823, 1606, 1325, 1126, 750 cm⁻¹; ¹H NMR (500 MHz, CDCl₃) δ 2.59–2.61 (m, 4H, pip-H), 3.54–3.56 (m, 6H, CH₂, pip-H), 7.29–7.32 (m, 4H, Ar-H), 7.74 (d, J = 1.50 Hz, 1H, Py-H), 8.38 (s, 1H, Py-H); EI-MS, m/z (%) 389 (6, M⁺), 340 (4), 209 (11), 193 (14), 180 (56), 168 (10), 125 (100), 56 (13). HRMS (EI⁺) calcd for C₁₇H₁₆Cl₂F₃N₃, 389.0673; found, 389.0665.

1-(2,6-Difluorobenzyl)-4-[3-chloro-5-(trifluoromethyl)pyridin-2-yl]piperazine (B₆): yield, 75%; yellow solid; mp, 43–45 °C; IR (KBr) ν 2844, 1611, 1314, 1134, 785 cm⁻¹; ¹H NMR (500 MHz, CDCl₃) δ 2.67–2.69 (m, 4H, pip-H), 3.53–3.55 (m, 4H, pip-H), 3.79 (s, 2H, CH₂), 6.91–6.93 (m, 2H, Ar-H), 7.26–7.27 (m, 1H, Ar-H), 7.72 (d, J = 2.00 Hz, 1H, Py-H), 8.37 (s, 1H, Py-H); EI-MS, m/z (%) 391 (18, M⁺), 372 (12), 221 (12), 195 (33), 182 (100), 170 (25), 127 (74). HRMS (EI⁺) calcd for C₁₇H₁₅ClF₅N₃, 391.0875; found, 391.0861.

1-(Pyridin-3-ylmethyl)-4-[3-chloro-5-(trifluoromethyl)pyridin-2-yl]piperazine (B₇): yield, 69%; yellow oil; IR (KBr) ν 2792, 1597, 1324, 1123, 760 cm⁻¹; ¹H NMR (500 MHz, CDCl₃) δ 2.62–2.64 (m, 4H, pip-H), 3.54–3.56 (m, 4H, pip-H), 3.60 (s, 2H, CH₂), 7.28–7.29 (m, 1H, Py-H), 7.73–7.75 (m, 2H, Py-H), 8.39 (s, 1H, Py-H), 8.54 (d, J = 4.00 Hz, 1H, Py-H), 8.58 (s, 1H, Py-H), 8.54 (d, J = 4.00 Hz, 1H, Py-H), 8.58 (s, 1H, Py-H). EI-MS, m/z (%) 356 (4, M⁺), 209 (10), 180 (7), 160 (15), 147 (100), 135 (10), 93 (42), 56 (11); HRMS (EI⁺) calcd for C₁₆H₁₆ClF₃N₄, 356.1016; found, 356.1021.

1-(6-Chloropyridin-3-ylmethyl)-4-[3-chloro-5-(trifluoromethyl)pyridin-2-yl]piperazine (B₈): yield, 76%; yellow oil; IR (KBr) ν 2803, 1597, 1449, 1310, 1128, 749 cm⁻¹; ¹H NMR (500 MHz, CDCl₃) δ 2.59–2.61 (m, 4H, pip-H), 3.52–3.54 (m, 4H, pip-H), 3.56 (s, 2H, CH₂), 7.32 (d, J = 8.10 Hz, 1H, Py-H), 7.70 (d, J = 7.17 Hz, 1H, Py-H), 7.75 (d, J = 1.84 Hz, 1H, Py-H), 8.35 (d, J = 1.95 Hz, 1H, Py-H), 8.39 (s, 1H, Py-H); EI-MS, m/z (%) 390 (7, M⁺), 221 (13), 209 (58), 194 (47), 181 (100), 126 (89), 56 (13). HRMS (EI⁺) calcd for C₁₆H₁₅Cl₂F₃N₄, 390.0626; found, 390.0628.

1-[(2-Chlorothiazol-5-yl)methyl]-4-[3-chloro-5-(trifluoromethyl)pyridin-2-yl]piperazine (B₉): yield, 72%; yellow oil; IR (KBr) ν 2823, 1597, 1316, 1126, 750 cm⁻¹; ¹H NMR (500 MHz, CDCl₃) δ 2.64–2.66 (m, 4H, pip-H), 3.52–3.54 (m, 4H, pip-H), 3.72 (s, 2H, CH₂), 7.38 (s, 1H, thiazol-H), 7.74–7.75 (m, 1H, Py-H), 8.39 (s, 1H, Py-H); EI-MS, m/z (%) 396 (7, M⁺),

361 (24), 223 (29), 209 (76), 187 (53), 165 (33), 145 (16), 131 (100), 56 (21). HRMS (EI+) calcd for $C_{14}H_{13}Cl_2F_3N_4S$, 396.0190; found, 396.0200.

1-(4-Chlorobenzyl)-4-[6-chloro-5-(trifluoromethyl)pyridin-2-yl]piperazine (B₁₀): yield, 46%; yellow oil; IR (KBr) ν 2808, 1601, 1329, 1129, 805 cm^{-1} ; 1H NMR (500 MHz, $CDCl_3$) δ 2.51–2.53 (m, 4H, pip-H), 3.54 (s, 2H, CH_2), 3.64–3.66 (m, 4H, pip-H), 6.47 (d, $J = 8.80$ Hz, 1H, Py-H), 7.29–7.32 (m, 4H, Ar-H), 7.67 (d, $J = 8.80$ Hz, 1H, Py-H); EI-MS, m/z (%) 389 (54, M^+), 370 (11), 264 (17), 223 (18), 209 (25), 180 (100), 168 (39), 125 (83). HRMS (EI+) calcd for $C_{17}H_{16}Cl_2F_3N_3$, 389.0673; found, 389.0673.

1-(2,3-Dichlorobenzyl)-4-[6-chloro-5-(trifluoromethyl)pyridin-2-yl]piperazine (B₁₁): yield, 47%; yellow oil; IR (KBr) ν 2823, 1617, 1319, 1113, 769 cm^{-1} ; 1H NMR (500 MHz, $CDCl_3$) δ 2.61–2.63 (m, 4H, pip-H), 3.65–3.69 (m, 6H, CH_2 , pip-H), 6.48 (d, $J = 8.40$ Hz, 1H, Py-H), 7.22 (m, 1H, Ar-H), 7.41–7.42 (m, 2H, Ar-H), 7.68 (d, $J = 8.00$ Hz, 1H, Py-H); EI-MS, m/z (%) 423 (22, M^+), 404 (21), 388 (19), 264 (14), 243 (29), 214 (100), 158 (79), 123 (8). HRMS (EI+) calcd for $C_{17}H_{15}Cl_3F_3N_3$, 423.0284; found, 423.0288.

1-[(6-Chloropyridin-3-yl)methyl]-4-[6-chloro-5-(trifluoromethyl)pyridin-2-yl]piperazine (B₁₂): yield, 46%; yellow solid; mp, 98–99 °C; IR (KBr) ν 2810, 1611, 1315, 1123, 750 cm^{-1} ; 1H NMR (500 MHz, $CDCl_3$) δ 2.52–2.54 (m, 4H, pip-H), 3.54 (s, 2H, CH_2), 3.64–3.65 (m, 4H, pip-H), 6.50 (d, $J = 8.79$ Hz, 1H, Py-H), 7.33 (d, $J = 8.08$ Hz, 1H, Py-H), 7.66–7.68 (m, 2H, Py-H), 8.34 (d, $J = 2.17$ Hz, 1H, Py-H); EI-MS, m/z (%) 390 (14, M^+), 221 (10), 209 (41), 194 (11), 181 (100), 169 (12), 126 (72), 56 (10). HRMS (EI+) calcd for $C_{16}H_{15}Cl_2F_3N_4$, 390.0626; found, 390.0633.

1-(2-Chlorothiazol-5-yl)methyl-4-[6-chloro-5-(trifluoromethyl)pyridin-2-yl]piperazine (B₁₃): yield, 46%; yellow oil; IR (KBr) ν 2806, 1593, 1316, 1126, 778 cm^{-1} ; 1H NMR (500 MHz, $CDCl_3$) δ 2.57–2.59 (m, 4H, pip-H), 3.63–3.65 (m, 4H, pip-H), 3.70 (s, 2H, CH_2), 6.47 (d, $J = 8.66$ Hz, 1H, Py-H), 7.38 (s, 1H, thiazol-H), 7.68 (d, $J = 8.66$ Hz, 1H, Py-H); EI-MS, m/z (%) 396 (12, M^+), 361 (37), 223 (40), 209 (82), 187 (61), 175 (24), 165 (11), 153 (15), 145 (15), 131 (100), 56 (37). HRMS (EI+) calcd for $C_{14}H_{13}Cl_2F_3N_4S$, 396.0190; found, 396.0196.

1-(2,6-Difluorobenzyl)-4-[6-chloro-5-(trifluoromethyl)pyridin-2-yl]piperazine (B₁₄): yield, 44%; white solid; mp, 65.0–65.9 °C; IR (KBr) ν 2886, 1613, 1314, 1122, 791 cm^{-1} ; 1H NMR (500 MHz, $CDCl_3$) δ 2.62–2.64 (m, 4H, pip-H), 3.67–3.69 (m, 4H, pip-H), 3.83 (s, 2H, CH_2), 6.45 (d, $J = 8.80$ Hz, 1H, Py-H), 6.94–6.95 (m, 2H, Ar-H), 7.29 (m, 1H, Ar-H), 7.66 (d, $J = 8.80$ Hz, 1H, Py-H); EI-MS, m/z (%) 391 (19, M^+), 264 (13), 221 (10), 182 (100), 127 (76), 56 (2). HRMS (EI+) calcd for $C_{17}H_{15}ClF_5N_3$, 391.0875; found, 391.0870.

1-(4-Iodobenzyl)-4-[6-chloro-5-(trifluoromethyl)pyridin-2-yl]piperazine (B₁₅): yield, 45%; white solid; mp, 78.8–79.7 °C; IR (KBr) ν 2813, 1593, 1321, 1129, 791 cm^{-1} ; 1H NMR (500 MHz, $CDCl_3$) δ 2.52–2.54 (m, 4H, pip-H), 3.52 (s, 2H, CH_2), 3.64–3.66 (m, 4H, pip-H), 6.47 (d, $J = 8.80$ Hz, 1H, Py-H), 7.11–7.13 (m, 2H, Ar-H), 7.69 (m, 3H, Ar-H, Py-H); EI-MS, m/z (%) 481 (23, M^+), 285 (11), 272 (87), 260 (31), 216 (100), 209 (8). HRMS (EI+) calcd for $C_{17}H_{16}ClF_3IN_3$, 481.0030; found, 481.0031.

1-(4-tert-Butylbenzyl)-4-[6-chloro-5-(trifluoromethyl)pyridin-2-yl]piperazine (B₁₆): yield, 45%; white solid; mp, 111.5–112.1 °C; IR (KBr) ν 2806, 1600, 1321, 1113, 797 cm^{-1} ; 1H NMR (500 MHz, $CDCl_3$) δ 1.34 (s, 9H, $C(CH_3)_3$), 2.55–2.57 (m, 4H, pip-H), 3.57 (s, 2H, CH_2), 3.66–3.68 (m, 4H, pip-H), 6.46 (d, $J = 9.20$ Hz, 1H, Py-H), 7.28–7.29 (m, 2H, Ar-H), 7.37–7.38 (m, 2H, Ar-H), 7.66 (d, $J = 9.20$ Hz, 1H, Py-H); EI-MS, m/z (%) 411 (27, M^+), 264 (30), 202 (50), 190 (19), 147 (100), 117 (13), 56 (4). HRMS (EI+) calcd for $C_{21}H_{25}ClF_3N_3$, 411.1689; found, 411.1689.

1-(2-Chlorobenzyl)-4-[6-chloro-3-(trifluoromethyl)pyridin-2-yl]piperazine (B₁₇): yield, 24%; yellow oil; IR (KBr) ν 2826, 1587, 1302, 1103, 759 cm^{-1} ; 1H NMR (500 MHz, $CDCl_3$) δ 2.64–2.66 (m, 4H, pip-H), 3.44–3.46 (m, 4H, pip-H), 3.69 (s, 2H, CH_2), 6.88 (d, $J = 7.98$ Hz, 1H, Py-H), 7.22–7.23 (m, 2H, Ar-H), 7.36 (m, 1H, Ar-H), 7.53 (m, 1H, Ar-H), 7.74 (d, $J = 8.07$ Hz, 1H, Py-H); EI-MS, m/z (%) 389 (12, M^+), 209 (12), 180 (86), 168 (28), 125 (100), 56 (19). HRMS (EI+) calcd for $C_{17}H_{16}Cl_2F_3N_3$, 389.0673; found, 389.0700.

1-(2-Chloro-6-fluorobenzyl)-4-[6-chloro-5-(trifluoromethyl)pyridin-2-yl]piperazine (B₁₈): yield, 46%; yellow oil; IR (KBr) ν 2849, 1596, 1324, 1124, 780 cm^{-1} ; 1H NMR (500 MHz, $CDCl_3$) δ 2.65–2.67 (m, 4H, pip-H), 3.66–3.69 (m, 4H, pip-H), 3.79 (s, 2H, CH_2), 6.45 (d, $J = 8.80$

Hz, 1H, Py-H), 7.02 (m, 1H, Ar-H), 7.23–7.25 (m, 2H, Ar-H), 7.65 (d, $J = 8.80$ Hz, 1H, Py-H); EI-MS, m/z (%) 407 (18, M^+), 264 (11), 221 (14), 198 (100), 186 (44), 143 (82), 42 (6). HRMS (EI+) calcd for $C_{17}H_{15}Cl_2F_4N_3$, 407.0579; found, 407.0579.

1-(3-Chlorobenzyl)-4-[6-chloro-5-(trifluoromethyl)pyridin-2-yl]piperazine (B₁₉): yield, 47%; yellow oil; IR (KBr) ν 2823, 1611, 1308, 1134, 780 cm^{-1} ; 1H NMR (500 MHz, $CDCl_3$) δ 2.54–2.56 (m, 4H, pip-H), 3.55 (s, 2H, CH_2), 3.66–3.68 (m, 4H, pip-H), 6.47 (d, $J = 8.80$ Hz, 1H, Py-H), 7.26–7.28 (m, 3H, Ar-H), 7.39 (s, 1H, Ar-H), 7.67 (d, $J = 8.80$ Hz, 1H, Py-H); EI-MS, m/z (%) 389 (29, M^+), 264 (13), 221 (16), 209 (22), 180 (100), 168 (34), 125 (63), 42 (6). HRMS (EI+) calcd for $C_{17}H_{16}Cl_2F_3N_3$, 389.0673; found, 389.0673.

1-(2-Chlorobenzyl)-4-[6-chloro-5-(trifluoromethyl)pyridin-2-yl]piperazine (B₂₀): yield, 51%; yellow oil; IR (KBr) ν 2806, 1593, 1113, 750 cm^{-1} ; 1H NMR (500 MHz, $CDCl_3$) δ 2.59–2.61 (m, 4H, pip-H), 3.65–3.67 (m, 6H, CH_2 , pip-H), 6.46 (d, $J = 8.78$ Hz, 1H, Py-H), 7.23–7.25 (m, 2H, Ar-H), 7.36–7.37 (m, 1H, Ar-H), 7.50 (d, $J = 7.23$ Hz, 1H, Ar-H), 7.66 (d, $J = 8.81$ Hz, 1H, Py-H); EI-MS, m/z (%) 389 (M^+), 209 (12), 180 (86), 168 (28), 125 (100), 69 (10), 56 (19). HRMS (EI+) calcd for $C_{17}H_{16}Cl_2F_3N_3$, 389.0673; found, 389.0700.

1-(2,4-Dichlorobenzyl)-4-[6-chloro-5-(trifluoromethyl)pyridin-2-yl]piperazine (B₂₁): yield, 56%; yellow oil; IR (KBr) ν 2833, 1606, 1328, 1135, 804 cm^{-1} ; 1H NMR (500 MHz, $CDCl_3$) δ 2.58–2.60 (m, 4H, pip-H), 3.64–3.68 (m, 6H, CH_2 , pip-H), 6.48 (d, $J = 8.80$ Hz, 1H, Py-H), 7.26 (m, 1H, Ar-H), 7.41–7.43 (m, 2H, Ar-H), 7.68 (d, $J = 8.80$ Hz, 1H, Py-H); EI-MS, m/z (%) 423 (18, M^+), 264 (31), 214 (98), 202 (36), 158 (100), 123 (6), 56 (5). HRMS calcd for $C_{17}H_{15}Cl_3F_3N_3$, 423.0284; found, 423.0285.

1-[(6-Chloropyridin-3-yl)methyl]-4-phenylpiperazine (C₁): yield, 87%; white solid; mp, 135–136 °C; 1H NMR (500 MHz, $CDCl_3$) δ 2.63–2.65 (m, 4H, pip-H), 3.43–3.45 (m, 4H, pip-H), 3.69 (s, 2H, CH_2), 6.88 (d, $J = 7.98$ Hz, 1H, Py-H), 7.21–7.23 (m, 2H, Ar-H), 7.34–7.36 (m, 2H, Ar-H), 7.53 (m, 1H, Ar-H), 7.74 (d, $J = 8.07$ Hz, 1H, Py-H); EI-MS, m/z (%) 287 (100, M^+), 181 (16), 161 (52), 154 (42), 126 (64), 106 (68), 77 (44), 56 (52). HRMS (EI+) calcd for $C_{17}H_{16}Cl_2F_3N_3$, 287.1189; found, 287.1189.

1-[(6-Chloropyridin-3-yl)methyl]-4-[2,6-dinitro-4-(trifluoromethyl)phenyl]piperazine (C₂): yield, 79%; yellow solid; mp, 162–164 °C; IR (KBr) ν (cm^{-1}) 1540, 1321, 1156 cm^{-1} ; 1H NMR (500 MHz, $CDCl_3$) δ 2.54–2.56 (m, 4H, pip-H), 3.14–3.16 (m, 4H, pip-H), 3.55 (s, 2H, CH_2), 7.34 (d, $J = 8.07$ Hz, 1H, Py-H), 7.68 (s, 1H, Py-H), 8.03 (s, 2H, Ar-H), 8.32 (s, 1H, Py-H); EI-MS, m/z (%) 445 (1, M^+), 291 (5), 231 (7), 126 (100), 90 (8), 42 (11). HRMS (EI+) calcd for $C_{17}H_{15}ClF_3N_5O_4$, 445.0765; found, 445.0746.

Biological Assay. Larvae of the armyworm, *P. separata* (Walker), were reared continuously on freshly cut maize seedling under standard laboratory conditions (25 °C, 60% relative humidity, and a 16:8 h light/dark photoperiod). All compounds were dissolved in acetone and diluted with water containing Triton X-100 (0.1 $mg\ L^{-1}$) to 500 and 250 $mg\ L^{-1}$ in concentration for bioassay. Fresh leaves were dipped in diluted solutions of the chemicals for 5 s, and excess fluid was removed. Water containing Triton X-100 (0.1 $mg\ L^{-1}$) and acetone was used as control.

Effects on larval growth were assessed using second-instar larvae of the armyworm. After weighing, each batch of second-instar larvae of the armyworm ($n = 10$) was released on leaves. Controls were treated similarly. Each treatment was replicated three times. Larvae were reweighed after 120 h for every batch to count the growth inhibition. Mortality was assessed 72 h after treatment.

RESULTS AND DISCUSSION

Biological Activity. The biological activities against armyworm, *P. separata* (Walker), of the target compounds are summarized in **Table 2**. Most of the compounds **B₁–B₁₇** showed certain growth-inhibiting activities. Through careful observation, the treated larvae were found to decrease feeding compared to the control ones. It was also found that the bodies of the treated larvae were thinner and shorter than those of control ones, and the growth development of treated larvae lagged behind that of the control larvae. Generally, the symptoms induced by the target compounds were similar to those described for typical insect

Table 2. Biological Activities *I* (%) of Compounds **B**₁–**B**₂₁ against Armyworm

compd	R ₁	R ₂	<i>I</i> (%)
B ₁	4-chlorobenzyl	5-(trifluoromethyl)pyridin-2-yl	76.9 ^a
B ₂	(6-chloropyridin-3-yl)methyl	5-(trifluoromethyl)pyridin-2-yl	73.7 ^a
B ₃	(2-chlorothiazol-5-yl)methyl	5-(trifluoromethyl)pyridin-2-yl	48.4 ^a
B ₄	2-chlorobenzyl	3-chloro-5-(trifluoromethyl)pyridin-2-yl	78.6 ^a
B ₅	4-chlorobenzyl	3-chloro-5-(trifluoromethyl)pyridin-2-yl	55.5 ^a
B ₆	2,6-difluorobenzyl	3-chloro-5-(trifluoromethyl)pyridin-2-yl	36.6 ^a
B ₇	(pyridin-3-yl)methyl	3-chloro-5-(trifluoromethyl)pyridin-2-yl	78.6 ^a
B ₈	(6-chloropyridin-3-yl)methyl	3-chloro-5-(trifluoromethyl)pyridin-2-yl	83.5 ^a
B ₉	(2-chlorothiazol-5-yl)methyl	3-chloro-5-(trifluoromethyl)pyridin-2-yl	88.6 ^a
B ₁₀	4-chlorobenzyl	6-chloro-5-(trifluoromethyl)pyridin-2-yl	84.1 ^a
B ₁₁	2,3-dichlorobenzyl	6-chloro-5-(trifluoromethyl)pyridin-2-yl	51.2 ^a
B ₁₂	(6-chloropyridin-3-yl)methyl	6-chloro-5-(trifluoromethyl)pyridin-2-yl	25.4 ^a
B ₁₃	(2-chlorothiazol-5-yl)methyl	6-chloro-5-(trifluoromethyl)pyridin-2-yl	89.5 ^a
B ₁₄	2,6-difluorobenzyl	6-chloro-5-(trifluoromethyl)pyridin-2-yl	22.2 ^a
B ₁₅	4-iodobenzyl	6-chloro-5-(trifluoromethyl)pyridin-2-yl	13.7 ^a
B ₁₆	4- <i>tert</i> -butylbenzyl	6-chloro-5-(trifluoromethyl)pyridin-2-yl	30.0 ^a
B ₁₇	2-chlorobenzyl	6-chloro-3-(trifluoromethyl)pyridin-2-yl	74.8 ^a
B ₁₈	2-chloro-6-fluorobenzyl	6-chloro-5-(trifluoromethyl)pyridin-2-yl	27.5 ^b
B ₁₉	3-chlorobenzyl	6-chloro-5-(trifluoromethyl)pyridin-2-yl	100 ^b
B ₂₀	2-chlorobenzyl	6-chloro-5-(trifluoromethyl)pyridin-2-yl	93.3 ^b
B ₂₁	2,4-dichlorobenzyl	6-chloro-5-(trifluoromethyl)pyridin-2-yl	100 ^b
C ₁	(6-chloropyridin-3-yl)methyl	phenyl	0 ^a
C ₂	(6-chloropyridin-3-yl)methyl	2,6-dinitro-4-(trifluoromethyl)phenyl	14.9 ^a

^a Growth inhibiting activities at 500 mg L⁻¹, $P\% = 1 - T/D$ (D = the increased weight of the control larvae during 120 h; T = the increased weight of the treated larvae during 120 h). ^b Mortalities of the armyworm at 500 mg L⁻¹ ($P\%$) during 72 h. ^c Mortalities of the armyworm at 250 mg L⁻¹ ($P\%$) during 72 h.



Figure 1. Symptoms of poisoned armyworm induced by **B**₂₁ at 500 mg L⁻¹.

growth regulators. Interestingly, compounds **B**₁₈–**B**₂₁ exhibited distinctly different bioactivities from compounds **B**₁–**B**₁₇. They caused the armyworm's death within 72 h at 500 and 250 mg L⁻¹. It was found that the larvae could hardly move after eating the leaves containing the test substances (**B**₁₈–**B**₂₁), and the bodies remained spasmodic until the test larvae died as shown in **Figure 1**. The causation of the bioactivity difference between **B**₁₈–**B**₂₁ and **B**₁–**B**₁₇ is still under investigation.

Effect of N⁴-Aryl Group on Activities. To verify the effect of an N⁴-aryl group on activities, compounds **C**₁ and **C**₂ were prepared by replacing the trifluoromethylpyridinyl group on N⁴-substituents of **B**₂ with substituted phenyl groups. The bioassays showed that such replacement did weaken the growth-inhibiting activity, which demonstrated that a suitable N⁴-substituent, such as the trifluoromethylpyridinyl group, was significant for a compound to remain effective against the insect.

Quantitative Structure–Activity Relationship (QSAR). The relationship between growth-inhibiting activities and the structures of compounds **B**₁–**B**₁₇ was analyzed by a QSAR (Hansch) approach against physicochemical parameters. The computational work was accessed from the Drug Discovery

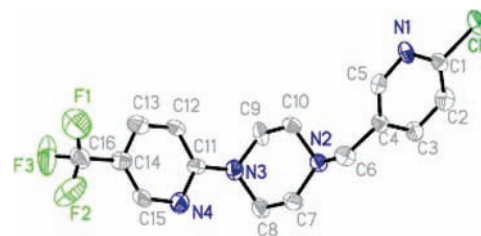


Figure 2. Crystal structure of compound **B**₂.

Workbench (DDW) module of Cerius² (version 4.8). The structures were minimized on the basis of the crystal structure of **B**₂ (**Figure 2**; the crystallographic data have been deposited at the Cambridge Crystallographic Data Centre in supplementary publication CCDC-658617. Copies of the data can be obtained, free of charge, at http://www.ccdc.cam.ac.uk/data_request/cif).

The data matrix was analyzed by the partial least-squares (PLS) method. The quality of each of the regression models was evaluated using the square of the correlation coefficient (r^2), cross-validation squared correlation coefficient (XVr^2), and predicted sum of squares (PRESS). The cross-validation squared correlation coefficient XVr^2 was used to measure the predictive ability of the equation (13, 14).

To find out which parameters are more important to activity, several equations were obtained according to the different combinations of the parameters. The most significant combination of physicochemical parameters affecting activity were $\log P(o/w)$, PEOE_VSA-1, and vsa_hyd, which were calculated by MOE (15, 16) presented in **Table 3**. The growth inhibiting activity data (% *I*) at 500 mg L⁻¹ were converted to $\log\{I/[(100 - I) \times MW]\}$ (17) as a dependent parameter, X .

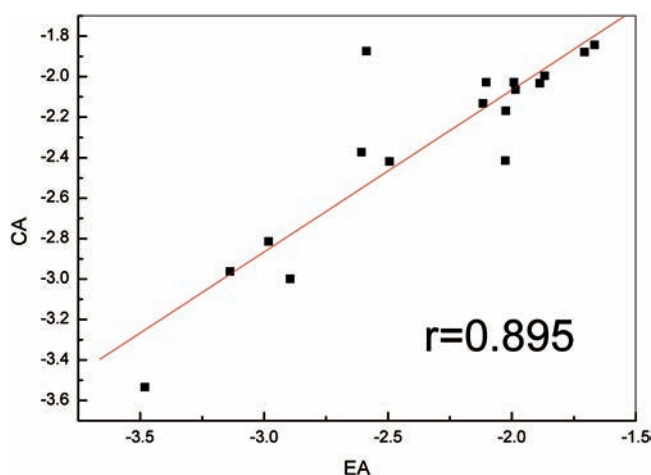
$$X = \log\{I/[(100 - I) \times MW]\}$$

The physical parameters $\log P(o/w)$, PEOE_VSA-1, and vsa_hyd are the independent variables of the regression, and

Table 3. Experimental Activities, Calculated Activities, and Physicochemical Parameters of Compounds **B**₁–**B**₁₇

compd	I%	X ^a	calcd ^b	log P(o/w) ^c	PEOE_VSA-1 ^d	vsa_hyd ^e
B ₁	76.9	-2.027	-2.4145	3.83276	54.091755	299.9382
B ₂	73.7	-2.104	-2.02767	3.00476	41.836849	284.101
B ₃	48.4	-2.587	-1.87392	2.69176	33.766548	274.2206
B ₄	78.6	-2.025	-2.16922	4.45776	95.928604	318.2314
B ₅	55.5	-2.494	-2.41951	4.45976	83.673698	318.2314
B ₆	36.6	-2.894	-2.99858	4.16976	41.836849	310.1802
B ₇	78.6	-1.986	-2.06364	2.63476	41.836849	293.1117
B ₈	83.5	-1.887	-2.03269	3.63176	71.4188	302.3942
B ₉	88.6	-1.707	-1.87893	3.31876	63.348495	292.5139
B ₁₀	84.1	-1.868	-1.99634	4.00076	71.4188	293.3834
B ₁₁	51.2	-2.607	-2.37305	5.41676	113.25565	327.5138
B ₁₂	25.4	-1.992	-2.02729	3.00376	41.836849	284.101
B ₁₃	89.5	-1.667	-1.84258	3.68776	63.348495	283.5031
B ₁₄	22.2	-3.137	-2.96223	4.53876	41.836849	301.1694
B ₁₅	13.7	-3.481	-3.53444	5.42676	54.091755	325.1491
B ₁₆	30.0	-2.982	-2.81454	5.73576	134.84459	365.5528
B ₁₇	74.8	-2.117	-2.13287	4.82676	95.928604	309.2206

^a $X = \log\{I/[(100 - I) \times MW]\}$ (I% = growth-inhibiting activities at 500 mg L⁻¹; MW = molecular weight). ^b The calculated activities. ^c Log P(o/w) = octanol/water partition coefficient. ^d PEOE_VSA-1 = van der Waals surface area of atomic partial charge $-0.10 \leq q \leq -0.05$. ^e vsa_hyd = approximate van der Waals surface area of hydrophobic atoms.

**Figure 3.** Relationship between the experimental activities (EA) and the calculated activities (CA).

X is the dependent variable.

$$X = -0.61955 + 0.01530(\text{PEOE}_V\text{SA-1}) - 0.67611 \log P(o/w) \quad (1)$$

$n = 17$, $r = 0.825$, $r^2 = 0.681$, $XVr^2 = 0.500$, and $\text{RMSE} = 0.295$.

Equation 1 is a divariant model with comparatively lesser r^2 and XVr^2 values.

$$X = 3.94200 + 0.02036(\text{PEOE}_V\text{SA-1}) - 0.38769 \log P(o/w) - 0.01991(\text{vsa}_{\text{hyd}}) \quad (2)$$

$n = 17$, $r = 0.895$, $r^2 = 0.801$, $XVr^2 = 0.663$, and $\text{RMSE} = 0.233$.

As shown in **Figure 3**, higher values of r^2 and XVr^2 were observed with eq 2 in which X was correlated with log P(o/w), PEOE_VSA-1, and vsa_hyd. Therefore, eq 2 explained the activities of these compounds better than eq 1 and revealed that lower log P(o/w) and vsa_hyd values and higher PEOE_VSA-1

values could result in better bioactivities. In addition, log P(o/w) was found to be the most important factor for the activities.

Lower log P(o/w) suggested that the decrease of lipophilic property would strengthen the growth-inhibiting activity. This result suggested the introduction of a hydrophilic factor, such as the use of heterocyclic rings including oxygen and/or nitrogen might benefit the bioactivity of compounds. In agreement with the lower log P(o/w), lower vsa_hyd values meant the decrease of surface area of hydrophobic atoms in the molecule. A higher PEOE_VSA-1 value was associated with the increase of electronegative atoms in the molecule. Thus, the application of an electronegative atom or group (i.e., chlorine, fluorine, and trifluoromethyl group) would be encouraged for better bioactivity.

In conclusion, a series of 1-arylmethyl-4-[(trifluoromethyl)pyridin-2-yl]piperazine compounds derived from PAPP were synthesized, and their biological activities against armyworm were evaluated. By the preliminary bioassay, most of the target compounds exhibited certain growth-inhibiting activities or larvicidal activities against armyworm, *P. separata* (Walker). The results indicated that PAPP could become a lead compound for insecticides with novel modes of action. QSAR demonstrated that log P(o/w), PEOE_VSA-1, and vsa_hyd were the critical parameters for growth-inhibiting activities of target compounds. Further structural modification and biological evaluation are currently under investigation and will be reported in due course.

LITERATURE CITED

- Nässel, D. R. Serotonin and serotonin-immunoreactive neurons in the nervous system of insects. *Prog. Neurobiol.* **1988**, *30*, 1–85.
- Nässel, D. R. Neuropeptides, amine and amino acids in an elementary insect ganglion: functional and chemical anatomy of the unfused abdominal ganglion. *Prog. Neurobiol.* **1996**, *48*, 325–420.
- Osborne, R. H. Insect neurotransmission: neurotransmitter and their receptors. *Pharmacol. Ther.* **1996**, *69*, 117–142.
- Lange, A. B. A neurohormonal role for serotonin in the control of locust oviducts. *Arch. Insect Biochem. Physiol.* **2004**, *56*, 179–190.
- Puiroux, J.; Moreau, R.; Gourdoux, L. Variations of biogenic amine levels in the brain of *Pieris brassicae* pupae during nondiapausing and diapausing development. *Arch. Insect Biochem. Physiol.* **1990**, *14*, 57–69.
- Isabel, G.; Gourdoux, L.; Moreau, R. Change of biogenic amine levels in hemolymph during diapausing and non-diapausing status in *Pieris brassicae* L. *Comp. Biochem. Physiol. A* **2001**, *128*, 117–127.
- L'Helias, C.; Beaudry, P.; Callebert, J.; Launay, J. M. Head tryptophan hydroxylase activity and serotonin content during pre-metamorphosis of *Pieris brassicae*. *Biogenic Amines* **2001**, *16*, 497–522.
- Tierney, A. J. Structure and function of invertebrate 5-HT receptors: a review. *Comp. Biochem. Physiol. A* **2001**, *128*, 791–804.
- Smith, M. W.; Borts, T. L.; Emkey, R.; Cook, C. A.; Wiggins, C. J.; Gutierrez, J. A. Characterization of a novel G-protein coupled receptor from the parasitic nematode *H. contortus* with high affinity for serotonin. *J. Neurochem.* **2003**, *86*, 255–266.
- Tricklebank, M. D.; Forler, C.; Middlemiss, D. N.; Fozard, R. Tetrahydrobenzindoles: selective antagonists of the 5-HT₇ receptor. *J. Med. Chem.* **1999**, *42*, 533–535.
- Campiani, G.; Morelli, E.; Gemma, S.; Nacci, V.; Butini, S.; Hamon, M.; Novellino, E.; Greco, G.; Cagnotto, A.; Goegan, M.; Cervo, L.; Valle, F. D.; Fracasso, C.; Caccia, S.; Mennini, T. Pyrroloquinoxaline derivatives as high-affinity and selective 5-HT₃ receptor agonist: synthesis, further structure–activity relationships, and biological studies. *J. Med. Chem.* **1999**, *42*, 4362–4379.
- Kuipers, W.; Kruse, C. G.; van Wijngaarden, I.; Standaar, P. J.; Tulp, M. Th. M.; Veldman, N.; Spek, A. L.; Ijzerman, A. P. 5-HT_{1A}- versus D₂-receptor selectivity of flinnoxan and analogous N⁴-substituted N¹-arylpiperazines. *J. Med. Chem.* **1997**, *40*, 300–312.
- Cao, S.; Wei, N.; Zhao, C.; Li, L. N.; Huang, Q. C.; Qian, X. Syntheses, antifeedant activity, and QSAR analysis of new

- oxa(thia)diazolyl 3(2*H*)-pyridazinones. *J. Agric. Food Chem.* **2005**, *53*, 3120–3125.
- (14) Yang, G.-F.; Huang, X. Development of quantitative structure–activity relationships and its application in rational drug design. *Curr. Pharm. Design* **2006**, *12*, 4601–4611.
- (15) Godden, J. W.; Bajorath, J. An information-theoretic approach to descriptor selection for database profiling and QSAR modeling. *QSAR Comb. Sci.* **2003**, *22*, 487–497.
- (16) MOE 2005.6. Chemical Computing Group Inc.
- (17) Zhu, Y. Q.; Liu, P.; Si, X. K.; Zou, X. M.; Liu, B.; Song, H. B.; Yang, H. Z. A quantitative structure-activity relationship study of

herbicidal analogues of α -hydroxy-substituted 3-benzylidenepyrrolidene-2,4-diones. *J. Agric. Food Chem.* **2006**, *54*, 7200–7205.

Received for review July 29, 2009. Revised manuscript received October 20, 2009. Accepted November 19, 2009. Financial support from the National Key Project for Basic Research (Grant 2003CB114400), National Natural Science Foundation of China (Grant 20972052), Science and Technology Commission of Shanghai Municipality (Grant 08391911600), and Shanghai Leading Academic Discipline Project (Project B507) is gratefully acknowledged.